

Chapter 18

Advances in Neuroimaging for Neurodegenerative Disease

Michele Veldsman and Natalia Egorova

Abstract This chapter is intended as a primer to the most widely used neuroimaging methods available in the prediction, diagnosis and monitoring of the neurodegenerative diseases. We describe the imaging methods that allow us to examine brain structure, function and pathology and investigate neurodegenerative mechanisms in vivo. We describe methods to interrogate brain structure with magnetic resonance imaging (MRI), and brain function with molecular imaging, functional MRI and electro- and magneto-encephalography. We highlight the major neuroimaging advances, including brain stimulation and connectomics, which have brought new insights into a wide range of neurodegenerative diseases and describe some of the challenges in imaging clinical populations. Finally, we discuss the future of neuroimaging in neurodegenerative disease and its potential for generating predictive, diagnostic and prognostic biomarkers.

Keywords Magnetic resonance imaging • Molecular imaging • Electrophysiology • Connectomics • Neurodegeneration

Abbreviations

| | |
|-------|--|
| AD | Alzheimer's disease |
| aD | Axial diffusivity |
| BOLD | Blood oxygenation level dependent |
| bvFTD | Behavioural-variant fronto-temporal dementia |

M. Veldsman (✉)

Nuffield Department of Clinical Neuroscience, University of Oxford,
Level 6, West Wing, John Radcliffe Hospital, Oxford OX3 9DU, UK

The Florey Institute of Neuroscience and Mental Health, Melbourne Brain Centre,
245 Burgundy Street, Heidelberg, VIC 3084, Australia
e-mail: michele.veldsman@ndcn.ox.ac.uk

N. Egorova

The Florey Institute of Neuroscience and Mental Health, Melbourne Brain Centre,
245 Burgundy Street, Heidelberg, VIC 3084, Australia

| | |
|-------|--|
| CBD | Cortico-basal syndrome |
| CT | Computed tomography |
| DBS | Deep brain stimulation |
| DTI | Diffusion tensor imaging |
| DWI | Diffusion weighted imaging |
| EEG | Electroencephalography |
| ERP | Event-related potential |
| FA | Fractional anisotropy |
| FDG | Fluorodeoxyglucose |
| FLAIR | Fluid attenuated inversion recovery |
| fMRI | Functional magnetic resonance imaging |
| HD | Huntington's disease |
| HMPAO | Hexamethylpropyleneamine oxime |
| ICA | Independent components analysis |
| MCI | Mild cognitive impairment |
| MEG | Magnetoencephalography |
| MRA | Magnetic resonance angiography |
| MRI | Magnetic resonance imaging |
| MS | Multiple sclerosis |
| NAA | <i>N</i> -Acetylaspartate |
| PD | Parkinson's disease |
| PET | Positron emission tomography |
| PNFA | Primary non-fluent aphasia |
| rD | Radial diffusivity |
| SD | Semantic dementia |
| SPECT | Single-photon emission computed tomography |
| SUV | Standardised uptake value |
| T | Tesla |
| TES | Transcranial electrical stimulation |
| TMS | Transcranial magnetic stimulation |

18.1 Introduction

Over the last two decades, technical developments in imaging hardware, advanced analysis methods and the growth of computing power have allowed us to non-invasively map the human brain in incredible detail, quantifying tissues and pathologies that were once only accessible at autopsy. We now have tools available to image the brain at different spatial and temporal scales across the lifespan and pre-symptomatically in neurodegenerative disease. These advances allow us to detect the earliest stages of many pathological processes, tracking their progression through the course of disease.

Neuroimaging allows *in vivo* insight into brain structure, function and pathology. Perhaps the most widely used imaging tools for neurodegenerative disease are molecular imaging and magnetic resonance imaging (MRI). Magnetic resonance imaging is particularly versatile in imaging brain structure, allowing estimation of brain volume, cortical thickness, white matter connectivity and tissue microstructure from three-dimensional images acquired without ionising radiation. Major technical advances in MRI have allowed increasingly high resolution scanning of brain structure and function from magnetic field strength of 0.5 tesla (T) to 3T, which is now widely used in clinical research. Scanners now have wider bores, allowing greater patient comfort and tolerance. Ultra-high field MRI scanners are becoming more common in research centres, and there are now over fifty 7T scanners around the world. This technical development allows imaging of subcortical structures and vasculature not previously visible on MRI.

Molecular imaging, including Positron Emission Tomography (PET) and single-photon emission computed tomography (SPECT), enables imaging of many aspects of brain function including brain metabolism, blood flow, neurotransmitter activity and pathological protein deposition. In nuclear medicine, highly specific tracers are being developed to image the by-products of pathological processes including activated microglia, amyloid plaques and neurofibrillary tangles. MRI can also be used to image brain function, allowing estimation of brain activity reflected in blood oxygenation and blood perfusion. These techniques are not mutually exclusive, with PET/MR systems combining the best aspects of both techniques.

Beyond the core MRI and molecular imaging methods, there are techniques that image almost all aspects of brain function. Electroencephalography (EEG) and magnetoencephalography (MEG) measure electric and magnetic fields generated by synchronised neuronal activity. EEG and MEG can record activity associated with a time-locked response to a sensory, cognitive or motor event at high temporal resolution as well as ongoing spontaneous oscillatory activity. Combining imaging modalities with new analytic methods provides a particularly powerful way of studying the brain in neurodegenerative disease. Finally, brain stimulation targeting specific brain structures and networks is going beyond neuroimaging by modulating brain function. Brain stimulation can inform theories of brain function by demonstrating a causal link between structure and function. A major advance in neuroimaging has been the emergence of the field of connectomics which seeks to describe the complex architecture and connectivity of the brain. The field has the potential to clarify the spread of neurodegenerative disease in the brain.

Neurodegenerative diseases, including Alzheimer's disease (AD), Parkinson's disease (PD), Huntington's disease (HD) and epilepsy, have all benefited from neuroimaging in developing predictive biomarkers, describing pathological mechanisms and tracking the course of disease. In this chapter, we review acquisition and analysis methods for the techniques most relevant to imaging neurodegenerative disease as well as discuss important advances in the field. In doing this we will provide a methodological context for the preceding chapters as well as introduce new methods allowing us to characterise the degenerating brain.

18.2 Imaging Brain Structure

18.2.1 *Magnetic Resonance Imaging*

Magnetic resonance imaging is one of the most versatile imaging techniques, with sequences available to image brain activity, blood perfusion and the structure of grey matter, white matter, vasculature and pathological tissue. MRI takes advantage of the predictable behaviour of hydrogen protons inside of an externally applied magnetic field. Hydrogen is abundant in water and fat in the human body. Hydrogen atoms are magnetic due to the intrinsic spin of their single proton nuclei. Outside of a strong magnetic field, these protons spin on randomly oriented axes. When placed inside a strong magnetic field, most protons become aligned to it, and the net proton magnetisation cannot be distinguished from the external field. Radio frequency pulses are therefore applied to excite the nuclei causing them to precess (spin) in phase, changing the direction of their net magnetisation, perpendicular to the external magnetic field. The protons gradually return, relaxing into alignment with the outside magnetic field while resonating, or emitting, a detectable signal. Magnetic field gradients localise the resonant radio frequency signals in space. These smaller magnetic fields, applied linearly through space, disrupt the main magnetic field, causing protons at different regions of the imaged tissue to precess at different rates. Protons relax at different rates depending on their surrounding environment, meaning that the signal is different depending on the surrounding tissue. MRI scanner pulse sequences take advantage of the different spin excitation and relaxation times of protons in different tissue environments. This produces images of different contrasts, highlighting different tissue types or pathological states. Like pixels, which break up a 2D image into smaller elements, voxels break up MR images into volumetric elements. Many analysis methods in MRI are conducted on a voxel-wise basis, breaking the large multi-dimensional images into discrete elements for analysis.

18.2.2 *Brain Morphology*

Brain atrophy is a macroscale indicator of neurodegeneration. Structural scans are still routinely consulted by clinicians to localise atrophy as part of diagnosis of neurodegenerative diseases (Fig. 18.1a). Automated structural analysis methods now allow for quantifiable changes in brain anatomy, as the result of neurodegeneration, to be estimated within and across individuals. Brain regions can be segmented according to known anatomy, and features of their morphometry, such as their shape and volume, can be calculated. The gold standard remains manual segmentation (Fig. 18.1c) in which anatomists or highly trained researchers manually trace boundaries based on known anatomical landmarks. Advances in automated segmentation methods now allow multiple regions to be segmented automatically

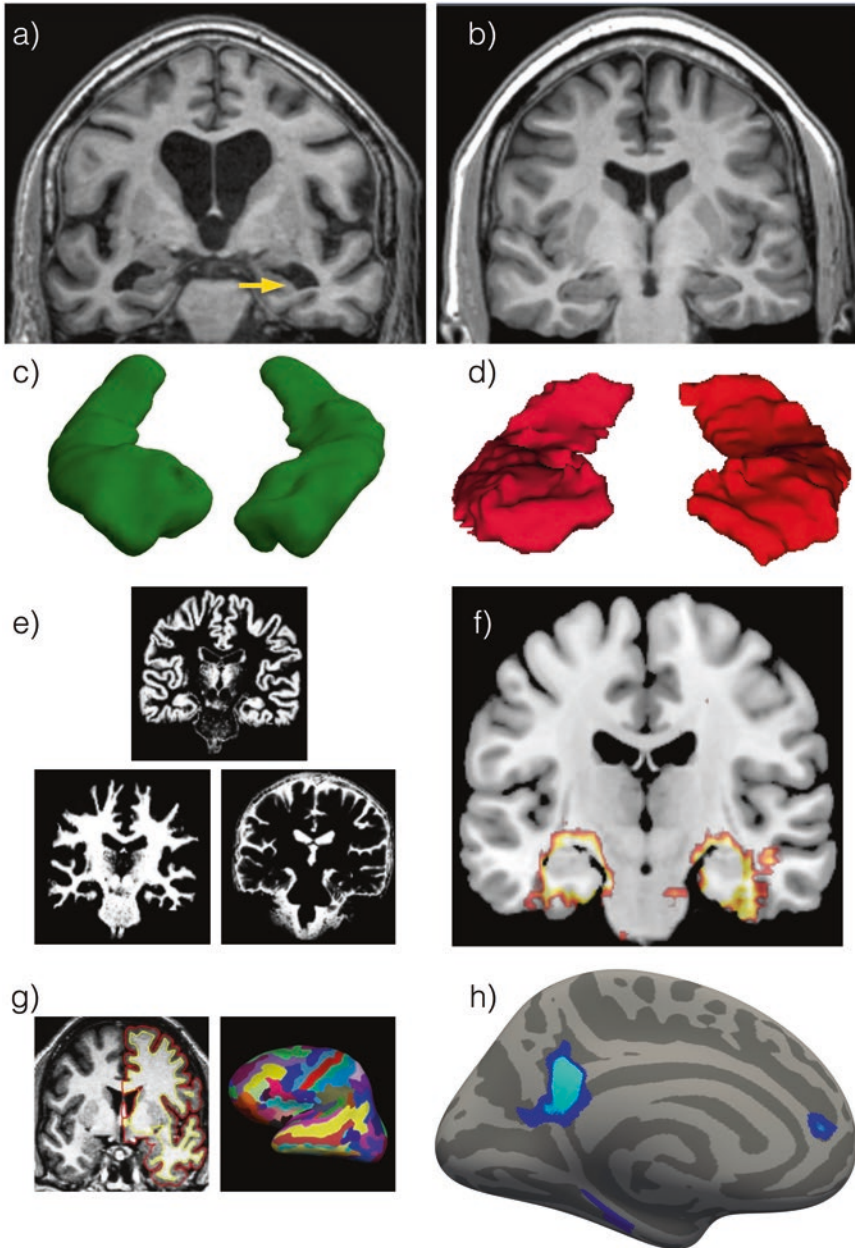


Fig. 18.1 Structural MRI Hippocampal atrophy in (a) Alzheimer's disease (highlighted by *yellow arrow*) compared to (b) healthy ageing; (c) manually segmented hippocampi, coronal orientation; (d) automated hippocampal segmentation using Freesurfer; (e) tissue segmentation of an anatomical image prior to voxel-based morphometry, showing (clockwise) grey matter, cerebrospinal fluid and white matter; (f) voxel-based morphometry: Representational statistical mapping showing greater medial temporal lobe atrophy in AD compared to healthy ageing; (g) surface based analysis: boundary between white matter and pial surfaces (*left*); probabilistic atlas used to label each point on the cortical surface; (h) regions showing statistically significant reduction in cortical thickness after ischaemic stroke rendered onto an inflated brain surface

according to probabilistic anatomical atlases (Fig. 18.1d). Automated structural segmentation methods are ideal for large cohort and longitudinal studies, saving many hours of manual work and ensuring consistency and reproducibility.

Structural analysis methods can be broadly divided into volume-based and surface-based methods. One of the most popular volume methods, voxel-based morphometry, normalises individual brains into a common brain template space. Cerebrospinal fluid, grey and white matter tissues are then segmented according to relative image intensities (Fig. 18.1e). The average grey matter density is compared across groups, using parametric statistical tests at every voxel [1], correcting for the vast number of statistical tests done across voxels. This analysis produces statistical maps showing local and global patterns of grey matter volume (Fig. 18.1f). Patient grey matter volume maps can be directly compared to volume maps of healthy individuals to show patterns of neurodegeneration [2]. Multiple regression and partial correlation methods can be used to correct statistical maps for confounding variables such as age, sex and handedness that may impact grey matter volume estimates independently of disease status.

In surface-based methods the boundary between grey matter and the inner white matter surface and between grey matter and the outer pial surface can be explicitly modelled (Fig. 18.1g). The distance between the inner and outer brain surfaces is calculated, taking into account complex cortical folding patterns. In contrast to volume-based methods that are based on relative image intensities, surface-based methods use cortical folding patterns to align individual surface anatomy to a template space (Fig. 18.1g). Surfaces from individuals are non-linearly registered to a cortical surface-based atlas of averaged folding patterns mapped onto a sphere [3]. Surface area and thickness can then be estimated and compared within and across individuals (Fig. 18.1h). Surface-based methods also allow for the estimation of shape, cortical folding and curvature patterns. Cortical thickness changes are seen in mild cognitive impairment (MCI), may help predict conversion to AD [4] and differentiate AD from frontotemporal dementia (FTD) [5].

Surface and volume-based methods can be used to show regional volume and cortical thickness changes and can also be used to estimate structural changes on a network-wide basis. Structural covariance describes patterns of correlations between regional estimates of brain morphology across populations [6] (Fig. 18.3b). Structural covariance methods have the potential to reveal principles of structural and functional brain development, organisation and degeneration in ageing and neurodegenerative disease [7].

A landmark paper by Seeley et al. (2009) demonstrated that the pattern of atrophy across five distinct neurodegenerative dementias closely resembled healthy functional networks and networks based on structural covariance [2]. They first investigated the pattern of atrophy in five dementia syndromes, AD, behavioural-variant fronto-temporal dementia (bvFTD), semantic dementia (SD), cortico-basal syndrome (CBS) and primary non-fluent aphasia (PNFA) using voxel-based morphometry and showed unique patterns of atrophy specific to each dementia syndrome. Taking the maximum point of atrophy in each syndrome as the seed, they explored structural and functional connectivity, relative to this seed region,

in healthy controls. They found a high correspondence between the patterns of atrophy in each dementia syndrome and healthy functional and structural covariance networks, indicating neurodegeneration was targeting specific and distributed networks in dementia syndromes. Importantly, they extended this work to provide a model of the transneuronal spread of neurodegenerative disease through healthy networks [8]. In temporal lobe epilepsy, patterns of atrophy also mirror healthy structural co-variance networks [9]. These results provide formal models based on MRI for why neurodegenerative pathologies may initially target a specific area of the brain and later spread to spatially distributed regions [8].

There are several benefits of structural imaging in neurodegenerative disease. It is non-invasive and often collected as part of routine clinical imaging. Images are quick to acquire and relatively easy to process. Several different analyses can be done on the same image and methods are highly automated, allowing large populations of patients to be compared. However, there are outstanding methodological issues that remain to be resolved. Structural images are affected by head motion [10], which can be particularly problematic in patient populations. A major hurdle in the use of structural imaging as a marker of neurodegeneration is the high degree of individual variability in brain structure. Longitudinal imaging overcomes this variability to a certain extent by allowing each person to act as their own control, so that changes in brain morphology can be tracked over time [11].

18.2.3 *White Matter*

18.2.3.1 **Diffusion MRI**

Diffusion MRI refers to MRI contrasts optimised for imaging white matter, including diffusion weighted imaging (DWI) and diffusion tensor imaging (DTI). When axons in white matter share a common destination, they often form larger bundles, or fibre tracts. Diffusion MRI is the only currently available technique for the estimation of the direction of these fibre tracts as well as tissue microstructure in vivo—changes in which often reflect neurodegenerative pathology [12].

Diffusion tensor imaging (DTI) models the degree and direction of diffusion of water molecules. Within fibre tracts, water molecules cannot diffuse symmetrically in all directions (isotropic diffusion), as they would in an unconstrained space, but rather they diffuse asymmetrically with preference along the length of fibres [12, 13]. Perpendicular to the length of the axon fibre, diffusion is more constrained, resulting in anisotropic diffusion. The architecture and integrity of the tissue as well as its orientation affect the diffusion of water molecules. The anisotropy of diffusion can be simply modelled with a 3×3 tensor, a mathematical description of the physical properties of the fibre architecture. The diffusion tensor is visualised as an ellipsoid, with its long axis oriented in the direction of the axis of greatest diffusion, the principle diffusion direction. For visualisation purposes, voxels can be colour coded

according to their principal diffusion direction, with red indicating diffusion along the *x*-axis (left-right), green along the *y*-axis (anterior-posterior) and blue along the *z*-axis (inferior-superior) (Fig. 18.3c).

Several measures of the degree and direction of diffusion can be made at a voxel-wise level. These measures can be compared between groups or correlated with behavioural or clinical variables. The measures can be overlaid onto anatomical images to represent or contrast structural integrity between groups or anatomical regions. The measures include the mean diffusivity (MD) and the apparent diffusion coefficient (ADC), a measure of the degree of displacement of water molecules; fractional anisotropy (FA) which is a summary measure of microstructural integrity; and axial and radial diffusivity (aD and rD), a measure of the rate of diffusion in the principal diffusion direction (aD) and perpendicular to the principal diffusion direction (rD). Fractional anisotropy is often used as a measure of structural integrity and is therefore of particular relevance in neurodegenerative disease. Mean diffusivity is increased in the amygdala, while the inferior longitudinal fasciculus (ILF) shows decreased FA in dementia with Lewy bodies. In contrast, AD patients show increased MD in medial temporal and parietal regions and decreased FA in the fornix, cingulum and ILF [14]. In HD, changes in FA, aD and rD are seen in presymptomatic HD and are more extensive in symptomatic HD [15]. Importantly, in both these populations, microstructural changes correlated with clinical variables suggesting a role for white matter changes in the cognitive symptoms observed in the diseases.

Diffusion tensor imaging is still the principal method for estimating white matter fibre connectivity in clinical populations. The simple tensor model was an elegant and simple solution to estimating white matter connectivity when first introduced, but it greatly oversimplifies white matter fibre architecture [12, 16]. Measurements are made on a voxel-wise level, with voxels around 1–2 mm in size. White matter fibres in comparison are around 1 μm in diameter. Therefore, a single voxel often contains tracts with many different fibres of different principle diffusion directions that cross, brush, branch, touch or fan out [16, 17]. DTI cannot adequately account for these situations, which may be the rule, rather than the exception, with evidence of multiple fibre orientations in over 90% of white matter voxels [16, 18]. Measures derived from the tensor model including FA, aD and rD are sensitive to the presence of crossing fibres [16]. For example, if a voxel contains tracts with two different principal diffusion directions, the FA value will be lower than if it contained a single tract and diffusion direction. The FA of both tracts are therefore underestimated. This confounding issue has important implications for the interpretation of FA as a proxy for white matter integrity as lower FA can be interpreted as reduced integrity, for example, across clinical populations, when it in fact reflects the presence of crossing fibres [16]. The solution to this problem has been offered by the fixel-based methods, taking into account individual fibre populations within each voxel ('fixels') [19].

18.2.3.2 Diffusion Tractography

The simplest form of tractography, deterministic tractography, uses line propagation techniques to estimate white matter pathways. A starting point is determined, for example, an anatomical point of interest, and criteria are set for when the tracking should be terminated. At its simplest, the principal diffusion direction in each voxel is taken as the orientation of the white matter tract and tract propagation is estimated by following the principal diffusion direction at consecutive steps from voxel to voxel. Deterministic algorithms provide a single direction for the orientation of white matter pathways at each step, without taking into account the uncertainty inherent in the estimation of the principal diffusion direction. In contrast, probabilistic tractography accounts for this uncertainty. Instead of estimating a single fibre orientation it estimates a probability distribution of fibre orientations. The tracking algorithm can then follow several different orientations according to their likelihood.

Diffusion tractography uses different models and algorithms to reconstruct fibre pathways based on estimates of fibre orientation in each voxel. Reconstruction of fibre pathways is therefore heavily dependent on scanning acquisition parameters and the algorithm used and should be considered a proxy for the white matter fibres, not a reconstruction of the fibres [12]. Deterministic and probabilistic approaches to tractography are the most popular techniques used in clinical settings, although momentum is growing for the use of more sophisticated acquisition techniques and algorithms that can better account for the complexity of white matter connections in the brain [16].

Despite having limitations to overcome and ongoing questions as to the biological validity of various tractography measures, the advantages of diffusion MRI are clear. The data can be acquired in relatively short scans and can be combined with other imaging modalities to provide validation of tracts. Although diffusion MRI provides important information of the orientation and direction of white matter fibre bundles, tissue microstructure can also be estimated from magnetisation transfer (MT) contrast MRI. MT uses off-resonance radio frequency pulses to contrast mobile, free water protons from protons bound to macromolecules, including proteins. MT can and has been used to investigate neurodegeneration and inflammation in the brain in AD and MS [20].

18.2.4 High-Resolution Structural Imaging

Ultra-high field imaging has potential to be an important neuroimaging tool for neurodegenerative disease. Ultra-high field imaging refers to the increased magnet strength of MRI, which at 7T, provides better image contrast and higher spatial resolution. Vasculature can be imaged at higher resolution, which is of relevance across neurodegenerative diseases including stroke, vascular dementia and AD. Subcortical structures are more easily delineated at 7T, allowing more precise

quantification of atrophy in structures including the basal ganglia, thalamic nuclei and hippocampal substructures [21].

High-resolution anatomical sequences have been developed specifically for clinical use, including Fluid-Attenuated Inversion Recovery (FLAIR) which is optimised for the detection of lesions in stroke and multiple sclerosis (MS) [22] and T2* weighted sequences optimised for the detection of microbleeds [23]. There is great promise for imaging the brain's vasculature with high-resolution MR angiography (MRA), including imaging smaller arteries, such as perforating lenticulostriate arteries that are not currently visible on lower resolution MRI [24]. Ultra-high field imaging is likely to improve the detection of white matter lesions or microbleeds which are pathological markers in vascular dementia [25]. Given the importance of the hippocampus in a range of neurodegenerative diseases, including AD, mild cognitive impairment and medial temporal lobe epilepsy, 7T imaging affords much greater anatomical detail of hippocampal substructures allowing detailed quantification of the shape, structure and connectivity of this important anatomical structure [21]. A grand aim for ultra-high field imaging is the detection of amyloid pathology, replacing the need for PET which involves ionising radiation and is less widely accessible than MRI. Early results in post-mortem brains are promising with hypointensities in T2* weighted imaging in regions corresponding to amyloid burden in AD, cerebral amyloid angiopathy and Down's syndrome [26].

Because of the higher field strength, patient safety, contraindication and tolerance is an issue in ultra-high field imaging for clinical populations. For example, certain aneurysm clips and compression screws considered safe at 3T are not safe at 7T [27]. Alongside the increasing magnet strength for MRI, has been the development of parallel acceleration sequences which allows higher resolution structural and functional imaging at 3T [28]. New pulse sequences, including multi-echo sequences, allow 3D volumes of the brain to be acquired simultaneously, shortening scan time and increasing signal-to-noise and contrast-to-noise ratio. These advances may fill the gap between low patient tolerance and safety exclusions at 7T and the need for higher resolution and faster sequences at 3T. A recent review of structural imaging methods for MRI is recommended for a comprehensive evaluation of the potential and pitfalls of imaging neuroanatomy with MRI [28].

18.3 Imaging Brain Function

18.3.1 *Functional MRI*

Functional magnetic resonance imaging (fMRI) utilises the blood oxygenation level dependent (BOLD) contrast to image the flow of blood to metabolically active areas of the brain. When neurons become active, their oxidative metabolic rate increases, which results in increased supply of oxygenated haemoglobin and a respective decrease in the amount of deoxygenated haemoglobin [29]. Deoxygenated

haemoglobin is paramagnetic and oxygenated haemoglobin is diamagnetic. Therefore, veins and capillaries containing deoxygenated blood distort the magnetic field in the vicinity, while vessels containing oxygenated arterial blood cause little or no distortion to the magnetic field, thus producing measurable signal in fMRI [30, 31]. BOLD fMRI benefits from high spatial resolution with a temporal resolution of a few seconds.

18.3.1.1 Task fMRI

Task fMRI relies on the hemodynamic response, the delivery of oxygen and glucose by blood in response to transient increases in activity. The dominant model of the haemodynamic response is characterised by an initial dip [32] as oxygen is depleted in the surrounding vasculature, this is followed by an increase in the oxy/deoxyhaemoglobin ratio resulting in higher MR signal peaking around 5 s following the stimulus onset. After the peak it plateaus (if the stimulus is maintained for longer) and returns to the baseline around 12–15 s later, but eventually decreases even further — an undershoot effect — before returning to the baseline [33].

Measures of activation level, extent or intensity (hypo- or hyper-activation) can be used to estimate in vivo processing of various cognitive and motor tasks (Fig. 18.2b). When imaging neurodegenerative disease, these measures are compared with the neural response in control groups to assess functional changes associated with the disease. In some cases functional changes that can be measured with fMRI precede structural changes and performing a task specifically affected by the disease is the strongest predictor of decline [34]. For example, separate cohorts of Huntington's disease gene mutation carriers and control participants performed four different tasks in the scanner, probing functions either primarily affected by the disease (i.e. motor control), higher cognitive functions (i.e. working memory and irritability), or basic sensory functions (i.e. auditory system). Best classification of patients and controls was achieved from fMRI-based activations with motor sequence tapping and task-induced irritation. Classification performance based on structural changes (grey matter probability maps) was also significantly above chance and similar to that of task fMRI. Both allowed separation of gene mutation carriers from controls with up to 80% accuracy on average 17 years before predicted disease onset [34]. In a similar way, fMRI was used to investigate spatial working memory in an N-BACK task (0, 1, and 2-BACK) in pre-manifest Huntington's disease, early symptomatic Huntington's disease, and control individuals. The lack of a robust striatal BOLD signal in pre-HD was observed and represented a very early signature of change detected up to 15 years prior to clinical diagnosis [35].

Task fMRI can also be used for identifying eloquent areas of the brain in pre-surgical evaluation in epilepsy [36]. Blood flow and volume increases reveal the eloquent areas involved in task or stimulus processing. This insight allows localisation of brain areas critical for certain functions and demarcates the boundaries of safe resection of areas adjacent to lesions. However, the technique has limitations,

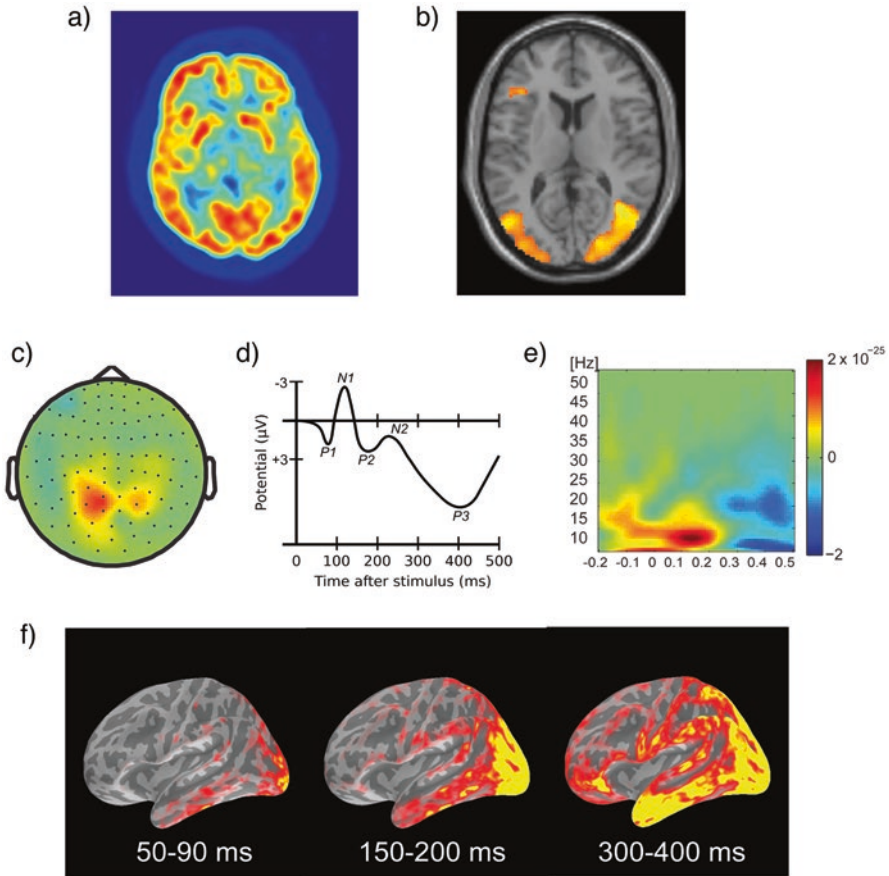


Fig. 18.2 (a) PET image showing accumulation (red areas) of tracer ^{18}F -FDG, axial slice; (b) fMRI statistical activation map, axial slice; (c) EEG topographic map; (d) Canonical event-related potential response; (e) time-frequency plot representative of an oscillatory analysis; (f) MEG source reconstruction showing activation dynamics over time

and false positive and negative results of fMRI warrant additional intraoperative electrocortical stimulation [37].

While fMRI is widely used in research involving healthy populations, the assumptions behind the modelling of the BOLD signal activity might not always hold in clinical populations. For example, the hemodynamic response to neural activity on which the BOLD signal is based may be altered due to perfusion and vasoreactivity changes as the result of ageing or ischaemic stroke [38]. BOLD signal changes in clinical populations may not reflect changes in neural activity, but rather changes in blood flow or blood volume as a result of ageing or pathology. Finally, there can be limitations on the use of functional tasks in clinical populations due to inability to perform the task at a required level or for a required duration. These methodological concerns have limited the translation of functional MRI in the clinic [34].

18.3.1.2 Resting-State fMRI

The alternative to using task fMRI in clinical populations is resting-state fMRI. A typical resting-state scan is acquired over 6–10 min with the subject keeping their eyes open or closed. It imposes no performance demands on patients who may have physical or cognitive impairments that prevent them from taking part in traditional task-based functional imaging. Resting-state fMRI is based on the intrinsic activity of the brain that can also be measured with BOLD contrast. This baseline activity, seen at rest, reflects spontaneous low-frequency fluctuations (<0.1 Hz) within distributed functionally specific networks. The same networks of regions that show correlated spontaneous activity at rest also show coordinated activity during specific tasks, suggesting they work together to coordinate sensory, motor, executive, affective and language functions [39, 40]. One of the most studied resting-state networks is the default mode network (DMN), comprising the posterior cingulate, medial pre-frontal cortex and the lateral and medial temporal cortex (Fig. 18.3a). The DMN is more active at rest [41, 42] and anti-correlated with the task-networks [43]. Reduced DMN connectivity has been consistently observed in AD [44] and is predictive of conversion of MCI to AD [45]. Key nodes of the DMN, including the posterior cingulate and inferior parietal lobes show hypometabolism and amyloid

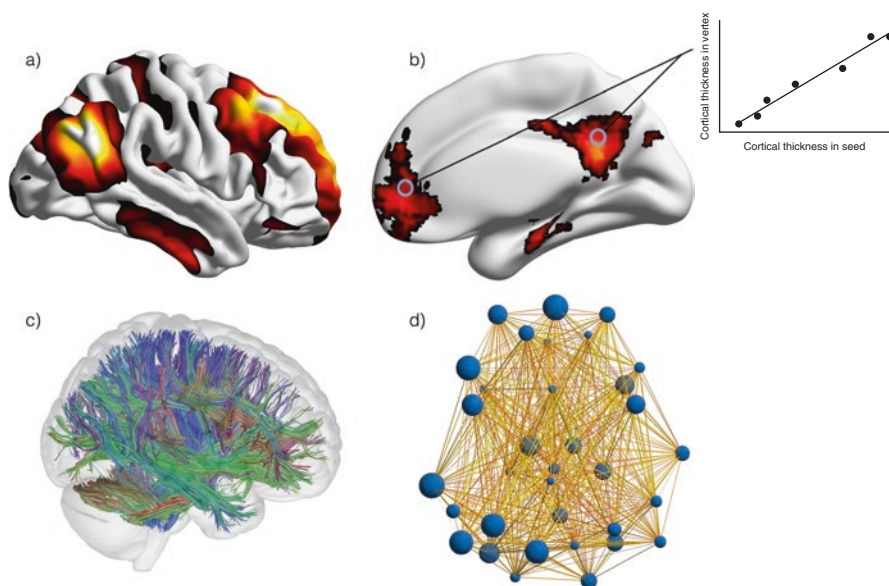


Fig. 18.3 (a) Default-mode network derived from resting-state MRI rendered on to a semi-inflated cortex, right lateral view; (b) representative structural covariance network showing correlations in cortical thickness with a seed region in the posterior cingulate, right medial view of inflated cortical surface; (c) whole brain diffusion tractography; (d) representation of a brain network. Nodes (blue) represent brain regions and edges (yellow) represent degree or strength of connectivity, axial viewpoint

deposition in AD [46]. Resting-state network connectivity has also been related to behavioural deficits in stroke, for example, spatial neglect is associated with connectivity changes in fronto-parietal networks [47].

Resting-state networks are often elucidated and described using functional connectivity methods that rely on establishing correlations in the time course of intrinsic fluctuations of spatially remote areas. Unlike anatomical connectivity, which considers physical connections and pathways that enable information exchange between different brain regions, functional networks do not need to be directly linked via white matter tracts. The primary methods for deriving functional connectivity networks are seed-based analysis and independent component analysis (ICA). Seed-based methods identify a relevant region of interest (ROI), a cluster of voxels or an anatomical region, and correlate the BOLD signal timecourse in the region with the BOLD signal timecourse in the rest of the voxels in the brain or a predefined set of ROIs [48]. Independent component analysis is a data driven method that detects resting-state networks by separating the signal in all voxels into spatially and temporally maximally independent components [49].

In addition to connectivity measures in the analysis of resting-state fMRI, other measures, such as the amplitude of low-frequency fluctuations, have been used. Measures of low frequency oscillations (LFO) in BOLD signal have been shown to reflect spontaneous neural functioning of the brain [50] and allow identifying changes in resting-state functioning without experimental tasks or a priori hypotheses. The method has proved to be sensitive to changes between clinical groups, including epilepsy [51], stroke [52] and MCI [53].

18.3.2 Molecular Imaging

Molecular imaging methods, such as PET and single-photon emission computed tomography (SPECT), allow imaging of brain function including cerebral blood flow, cerebral glucose metabolism and, perhaps most relevant to neurodegenerative disease, imaging of neuropathological depositions and markers of neuroinflammation. PET and SPECT also allow mapping of neurochemical processes, such as the density of postsynaptic receptors for various neurotransmitters (e.g., serotonin), presynaptic transporters for these transmitters, precursors (e.g., L-DOPA), and transmitter degrading enzymes [54]. New radio-compounds are being developed targeting tau, alpha-synuclein, cholinergic and dopaminergic transmission, and activated microglia and astrocytes as markers of neuroinflammation [55]. PET/MR systems combine the spatial resolution of MR with the direct imaging and quantification of neurodegenerative pathology of PET, providing potential for new biomarkers [56]. As PET has been extensively covered in other chapters, we provide only a brief introduction to the methods and recent advances.

18.3.2.1 Positron Emission Tomography

PET uses radioactively labelled short-lived tracers administered intravenously to image the brain. The tracers are made up of carrier molecules tightly bonded to an isotope. Carrier molecules interact or bind to specific proteins or sugars in the brain, depending on the biological process being tracked. The isotopes decay to produce particles called positrons which react with surrounding electrons and produce gamma rays. These gamma rays are detected by a gamma camera placed in close proximity to the head in the PET scanner [57]. This technology allows identification of the location and quantity of receptors and binding sites in the human brain.

Brain glucose metabolism can be measured using the radiotracer ^{18}F -Fluorodeoxyglucose (^{18}F -FDG; Fig. 18.2a). The uptake of ^{18}F -FDG can be semi-quantified using a standardised uptake value (SUV) and describes the ratio of tracer concentration, at a fixed point in time, relative to the injected dose of radiotracer given. ^{18}F -FDG has shown utility for differential diagnoses of dementias [58]. Patterns of glucose metabolism can differentiate Alzheimer's disease, dementia with Lewy bodies and frontotemporal dementia [59]. The use of ^{18}F -FDG as an imaging marker across neurodegenerative disease has been covered in previous chapters. It is perhaps most promising in its use as a marker of early hypometabolism in MCI, considered a precursor to AD [60]. Importantly, early evidence of hypometabolism is associated with cognitive impairment and predictive of conversion to AD, making ^{18}F -FDG a strong candidate biomarker for AD [60].

One of the most important advances in imaging methods for neurodegeneration was development of *in vivo* imaging of $\text{A}\beta$ -amyloid pathology in Alzheimer's disease which could previously only be evaluated at autopsy [61]. Imaging of amyloid pathology is now highly reliable, reproducible and routinely used to screen participants in clinical trials as well as evaluate drug effectiveness [61]. Molecular imaging has allowed for the detection of pathological hallmarks of Alzheimer's disease decades before clinical symptoms appear. The development of specific radiotracers for detection of a wider range of neurodegenerative pathologies is at the centre of molecular imaging research. Efforts have been focused on developing tracers that bind to pathological tau inclusion *in vivo* [61]. Pathological tau is associated with several neurodegenerative diseases, including frontotemporal dementia, motor neuron disease, progressive supranuclear palsy and corticobasal degeneration and chronic traumatic encephalopathy. Tau selective PET radiotracers are therefore of great utility as an imaging biomarker. There are a number of challenges in the development of radioligands. Tracers must be able to cross the blood brain barrier, have high affinity and selectivity to their target and have effective dosimetry [62]. For tau-PET, the tracer must also be able to cross cell membranes. A significant hurdle to the development of PET tracers is the short half-life of compounds, which require on-site, or at least nearby, cyclotrons for production.

18.3.2.2 Single Photon Emission Tomography

SPECT is a more accessible molecular imaging technique than PET, requiring lower cost equipment and using tracers with longer half-lives, avoiding the need for nearby or onsite cyclotrons. SPECT uses radioisotopes attached to a delivery compound to cross the blood-brain barrier once it is injected intravenously [63]. The most typically used isotopes in SPECT imaging have been technetium-99m (^{99m}Tc) and iodine-123 (^{123}I). Attaching ^{99m}Tc to hexamethylpropyleneamine oxime (HMPAO) or ethyl cysteinate dimer allows it to be taken up by brain tissue proportionally to brain blood flow. As blood flow in the brain is coupled with local metabolism, the ^{99m}Tc -HMPAO tracer metabolism allows the assessment of the cerebral blood flow. The spatial resolution of SPECT images is low, requiring the use of computed tomography (CT) or MRI for more precise spatial localisation. Unlike PET, SPECT cannot be performed in real time. Combined SPECT/CT and PET/CT scanners allow integrating 3D CT images and PET/SPECT data.

The measurement of cerebral blood flow in patients with cerebrovascular disease was the earliest application of SPECT in the brain [63]. SPECT imaging has been used in acute and chronic ischemia to define infarcted areas, and has recently been combined with diffusion imaging [64]. SPECT has been widely used for imaging of Alzheimer's disease, acute stroke, transient ischemic attacks, epilepsy and recurrent primary tumour [63]. Previous uses of SPECT imaging have also included imaging aromatic amino acid decarboxylase, which is involved in the synthesis of dopamine, norepinephrine, and serotonin and using dopamine transporter (DAT) ligands to evaluate changes in presynaptic DAT sites, particularly relevant for Parkinson's disease. Imaging with DAT ligand [^{123}I]FP-CIT (DaTSCAN) was found to reliably differentiate between PD and essential tremor patients [65].

18.3.2.3 Magnetic Resonance Spectroscopy

Magnetic resonance spectroscopy (MRS) is a non-invasive, non-ionising technique enabling the analysis of biochemical composition, the concentration of metabolites, of brain tissue. Different metabolites resonate at different frequencies, in line with standard MR physics principles, depending on their surrounding chemical environment.

MRS is sensitive to within-subject changes of concentration over time in the order of 1 mmol/L, giving an effective spatial resolution of 1–8 cm³. Typically, MRS is measured in a specific volume of interest. The MRS spectra show peaks representing a metabolite or group of metabolites ordered by the characteristic resonance frequency of its constituent nuclei. The most common nuclei are ^1H (proton), ^{23}Na (sodium) and ^{31}P (phosphorus). Proton spectroscopy provides higher signal-to-noise ratio and is most frequently used. The frequency of each peak is expressed in parts per million (ppm) of the resonant frequency of a reference metabolite [66].

Each metabolite appears at a specific ppm, and individually reflects specific cellular and biochemical processes. The brain metabolites that are commonly seen on

the MR spectrum are lactate resonating at 1.3 ppm, lipids at 1.3 ppm, *N*-acetylaspartate (NAA) at 2.0 ppm, glutamine/glutamate and GABA at 2.2–2.4 ppm, creatine at 3.0 ppm, choline at 3.2 ppm, myo-inositol at 3.5 ppm and water at 4.4 ppm. If raw signal was processed then the spectra would be dominated by water, which would make all other spectra invisible. Water suppression is therefore part of any MRS sequence, either via inversion recovery or chemical shift selective (CHESS). Different metabolites are associated with different physiological functions. For example, NAA, an amino acid derivative synthesised in the mitochondria of neural cells, is involved in myelin synthesis and is associated with viable neuronal axons and dendrites. NAA decreases with any disease that negatively affects neuronal integrity. Creatine provides a measure of energy stores. Myo-inositol, a sugar-alcohol, is often used as a marker of glial cell numbers. Lactate is a product of anaerobic glycolysis and is detectable in brain diseases where hypoxia is part of the differential, such as stroke and encephalopathy.

NAA, which is a marker of living neurons, has been shown to decline in AD, characterised by widespread neuronal loss, compared to MCI patients and healthy controls [67]. NAA decline is a sensitive measure and can be detected even when there is little decline in grey-matter volume [68]. Even before NAA decline, however, abnormal concentration of myo-inositol, which is present in glial cells, is observed [69]. The clinical specificity of one metabolite alteration in AD can be poor, but looking at a ratio of two metabolites increases diagnostic specificity and accuracy [66]. For example, a decrease in NAA/creatine ratio has been linked to the loss of synapses and early pTau pathology, whereas an increase in myo-inositol/creatine ratio is associated with the occurrence of amyloid-plaques [70].

18.4 Electro- and Magneto-Encephalography

Previously discussed functional methods are reliant on imaging blood flow, either directly or indirectly. The advantage of EEG and MEG is that they are the only non-invasive high-resolution imaging techniques that do not rely on relatively sluggish vascular responses but measure neurophysiology directly [71]. Active neurons produce electrical currents that propagate through the brain, reaching the scalp. The voltage differences that reach the scalp can be measured at the surface with EEG. The current inside the head also produces magnetic fields, which can be recorded above the scalp with MEG. MEG and EEG signal is mostly generated by the pyramidal neurons of the cortex, since they are arranged so that the apical dendrites are aligned perpendicularly to the cortical surface. These neurons behave as current dipoles, the activity of which can be detected by sensors on the surface of the skull. For the activity to be measurable, tens of thousands of neurons are required to be active synchronously [72].

Although measuring neural activity without relying on blood flow could be particularly important for disorders accompanied by vascular burden, EEG and MEG have limitations. For example, susceptibility to movement, lower spatial resolution

and reliability of the source reconstruction can be an issue. Both EEG and MEG reflect brain activity with millisecond temporal resolution, however, their spatial resolution is limited (between one and several centimetres), especially in comparison with haemodynamic imaging techniques. The topography of the signal measured at the surface of the scalp can be visualised by interpolating the signal between recording sites and creating colour-coded maps of activation (Fig. 18.2c). These maps only indicate approximate locations of the brain activity, although it is possible to estimate neural sources of the measured signal with more precision (Fig. 18.2f). It is important to note that both EEG and MEG suffer from what is called the ‘inverse’ problem, that is impossibility to unambiguously deduce the source currents responsible for the externally measured field. Even with an infinite amount of measurements around the head, no unique solution for the localisation of the sources of activity inside the head can be calculated, as only some features are uniquely determined and others need to be modelled based on various assumptions about the activity distribution. They can, nevertheless, be modelled quite accurately.

Although MEG and EEG lead fields are similar, EEG is sensitive to all primary currents, while MEG only records current flows tangential to the scalp. This means that MEG lead field is narrower. In addition, the potentials measured by EEG are smeared by the low conductivity skull. EEG recordings and localisation accuracy can also be affected by the electrode placement and the choice of the reference point. By contrast, MEG does not suffer from inhomogeneity of the volume conductor [73] and therefore it ‘sees’ a smaller area of the cortex (about 0.3 times that of the EEG), although localisation of the source is more accurate [74]. This increased precision makes MEG more useful for detecting a more restricted group of sources. Further gains can be made by combining simultaneous MEG and EEG recordings within the same experiment. EEG setup is much less expensive than MEG.

Although there are several differences between EEG and MEG, they can be analysed in a similar way. Event-related and resting-state analyses are analogous to those conducted for functional MRI. In addition, time-frequency resolved analysis of oscillatory neural activity can be performed for event-related and resting-state approaches.

18.4.1 Event-Related Analysis

Neurophysiological biomarkers can be based on specific brain responses to external stimuli. When the response to the stimulus is time-locked, an event-related potential (ERP) can be observed (Fig. 18.2d). To increase signal-to-noise ratio, multiple trials of the same response are recorded and then averaged. Response latencies with specific spatial distributions have been established for different cognitive processes. Well-studied components include P300 (indicating a positive deflection around 300 ms after stimulus onset) associated with attention and memory, and mismatch negativity (MMN) thought to reflect the mismatch between a trace in a sensory memory and the representation of the current stimulus to which the trace is compared. Response amplitude, latency and spatial distribution of ERPs can be compared

between experimental conditions and groups. In AD and schizophrenia both P300 and MMN have been used to characterise the disease and evaluate treatment [75]. For example, cognitive impairment in AD is associated with a reduction in ERP amplitude, delayed latency and altered spatial location of the MMN response. In healthy participants MMN is localised in the inferior frontal and superior temporal gyri, while in AD the strongest activity appears in parietal sites. For P300, generators are typically located in the frontal lobe for healthy control participants, but in AD they often shift to the temporal lobe. Reduction in inferior frontal source strength and the switch of the maximum intensity area to parietal and superior temporal sites suggest these areas may be of particular significance in neurodegenerative disorders implicating attention and memory [76].

18.4.2 Analysis of Induced and Resting-State Oscillations

Event-related activity reflects transient stimulus and time-locked changes in the brain. However, induced oscillatory activity (related to stimulation but not phase-locked) and spontaneous oscillatory activity in the absence of explicit stimulation can also be measured [77]. Oscillatory activity is typically divided into five frequency bands: the delta (0–3 Hz), theta (4–7 Hz), alpha (8–12 Hz), beta (13–30 Hz) and gamma (30–200 Hz) bands [78] (Fig. 18.2e). Each frequency band is associated with different spatial patterns and functions. Theta oscillations are largest over midline frontal regions and associated with working memory performance and focused attention [79]. Alpha activity is most prominent over centro-parietal and occipital cortex and associated with inhibitory function and attention [80]. Slow oscillations extend over larger brain areas, while high-frequency oscillations are typically more focused [81]. Coherence in the amplitude of fluctuations within a frequency band is thought to reflect functional connectivity between anatomically distant but functionally associated brain regions.

Alteration to oscillatory activity in PD has been well characterised. For example, simultaneous recording of MEG and local-field potentials from the subthalamic nucleus (STN) during deep-brain stimulation has revealed hyper-synchrony between STN neurons and cortical motor neurons. Theta and alpha band synchrony has been shown to correspond to the tremor frequency and harmonic, whereas beta and gamma synchrony is related to general motor deficits [71]. In addition, increased resting-state cortico-cortical functional connectivity in the 8–10 Hz alpha range has been documented in the early clinical stages [82]. With disease progression, connectivity is increased in the theta and beta bands [83], signalling topographical advancement of pathology over the brain.

18.5 Brain Connectivity

The field of MRI has advanced from analysing the structure and function of discrete brain regions, to the acceptance that the brain is organised into complex networks, with no single region working in isolation. Dysfunction or atrophy in specific

regions of the brain has long been associated with different neurodegenerative diseases. As the preceding chapters have outlined, hippocampal atrophy is a hallmark of AD, dopamine depletion of the substantia nigra is a hallmark of PD, and caudate and putamen dysfunction are characteristic of HD. However, these regions are embedded within complex brain circuitry, working in synchrony within a functional network of anatomically distributed regions and integrated into a complex structural network of axonal inputs and outputs. Even ischaemic stroke, traditionally thought to cause discrete damage within only the infarcted area, is now recognised as having widespread effects in the brain [84]. The field of connectomics has arisen as a result of recognition that the brain is best described in terms of its vast, complex and interconnected networks. These networks exist on multiple scales from a cellular to a systems level and can describe coordinated activity of distributed brain regions or the structural wiring that connects these regions. Several large-scale international projects have launched in the last decade attempting to formally characterise brain network function, including the Human Connectome Project [85] and the Human Brain Project [86].

Structural networks may describe either the brain's white matter connections (Fig. 18.3c) or patterns of covariations in morphological features of the brain (Fig. 18.3b). Functional networks refer to the coordinated activity of the brain, whether intrinsically or extrinsically initiated (Fig. 18.3a). Structural and functional networks are derived either by examining the relationship between a target, or seed region and the rest of the brain, or by using data driven approaches to decompose the brain into independent networks. The interaction within and between brain networks can be formally quantified with graph theory methods. Detailed reviews of network methodology in structural and functional imaging are available in the literature [87, 88]. Briefly, graph theory is a branch of network science that models different elements of the network (nodes) and the relationship between them (edges). Nodes may be anatomically or functionally defined regions and edges may describe a correlation in the timecourse of activity (as in functional network analysis) or some morphometric feature such as covariance in cortical thickness (Fig. 18.3d). Graph theory is an incredibly flexible and potentially powerful technique for formalising complex brain network changes in neurodegeneration. Brain regions can be classified as 'hubs' according to graph theory metrics, denoting their status within a network. Hubs are highly connected central nodes of a network. Network hubs have been shown to be disproportionately vulnerable to brain atrophy and pathology burden across neurological diseases [89]. For example, amyloid deposition is highest in network hub regions [90]. In a meta-analysis of voxel-based morphometry studies in over 20,000 patients, grey matter atrophy or lesions were more likely to be situated in network hubs than non-hub regions in over 26 neurological disorders, including schizophrenia and Alzheimer's disease [89]. Because hubs are high traffic, high metabolism areas, any blood flow, metabolic or pathological disturbance may have disproportionate effects on the network [91].

18.6 Brain Stimulation

With increasing recognition that complex brain networks are implicated in neurodegenerative disease, it becomes more challenging to find pharmacological interventions that are capable of altering brain circuit function. As a result, non-pharmacological interventions such as brain stimulation are showing great promise in the treatment of neurodegeneration, including deep brain stimulation for PD and transcranial magnetic stimulation (TMS) in stroke recovery. Brain stimulation methods can be broadly categorised into invasive and non-invasive methods; the former designed to stimulate small regions of tissue deep in the brain and necessitating surgical operation, the latter to temporarily disrupt or modulate cortical functions that do not require surgical intervention.

18.6.1 *Deep Brain Stimulation*

Deep brain stimulation (DBS) emerged in the 1990s as a neurosurgical intervention for relief of certain neurological conditions by the implantation of electrode arrays at target regions deep within the brain. An external device transmits electrical impulses to the implanted electrodes that stimulate the neurons at the target site. The amplitude and timing of the stimulation can be externally set, monitored and optimised for the patient and the site of stimulation. DBS was initially widely used for stimulation of the ventral intermediate thalamic nucleus as treatment for essential tremor [92]. DBS has since been shown to be an effective treatment of different symptoms of Parkinson's disease [93]. Stimulation of ventral intermediate thalamic nucleus eases tremor, while stimulation of the subthalamic nucleus improves gait and bradykinesia symptoms [92]. An expert consensus of DBS for PD concluded that it was an effective treatment for patients with medically intractable motor symptoms, or significant intolerance to drug treatment [93]. DBS has been trialled in other neurodegenerative disease including Huntington's disease [94, 95] and Alzheimer's disease [96]. Although results have been promising, trial numbers are still small and DBS has yet to be shown to be more effective than pharmacological treatment. DBS may be effective only in patients with medically intractable symptoms or in combination with pharmacological treatment [93].

18.6.2 *Transcranial Magnetic Stimulation*

The primary non-invasive methods available for the modulation of cortical function are transcranial magnetic stimulation (TMS) and transcranial electrical stimulation (TES). TMS is the more mature of the methods with more robust and well replicated supporting evidence, we will therefore focus on TMS, but the interested reader is

referred to Parkin et al. (2015) for an excellent primer on non-invasive brain stimulation [97]. In TMS, a coil is placed near the scalp, passing a magnetic field through the skull, which induces an electrical field in the underlying brain tissue. The frequency and intensity of the stimulation can be altered to excite or inhibit neuronal activity. Single pulse TMS has excitatory effects while repetitive TMS is used for inhibition of function. TMS can be combined with MRI and EEG to improve localisation of the target region for stimulation or examine network-wide effects of stimulation.

In the context of neurodegenerative disease, non-invasive brain stimulation is typically used to induce neuroplasticity with the aim of promoting recovery. Inducing plasticity is complex with variability in behavioural and neurophysiological response to stimulation dependent on age, sex, genetics and many other known and unknown variables in healthy subjects [98]. The use of TMS becomes more complex in neurological populations where there is also variability in pathology and disease phenotype. Nevertheless, there have been promising results, especially in the field of stroke, for the use of non-invasive brain stimulation for therapeutic purposes. TMS may help to constrain brain reorganisation after stroke (see [99] for a review of therapeutic use of TMS in stroke). Poor motor recovery is associated with increased compensatory contralesional hemispheric motor activity, and TMS has been shown to inhibit this activity, encouraging ipsilesional recovery of function [99]. The utility of TMS has been recognised for a number of neurological conditions, including stroke, epilepsy and schizophrenia, and led to the development of guidelines for therapeutic use [100].

18.7 Trends and Future Directions in Neuroimaging

There is no one size fits all for imaging the brain in neurodegenerative disease. The wide range of pathologies underlying different neurodegenerative disorders are matched by a wide range of neuroimaging techniques and analysis methods. In many cases, a combination of methods is ideal and allows characterisation of brain structure and function at different scales, with each modality informing and constraining models based on other modalities. Recognition that biomarkers are unlikely to come from neuroimaging alone, let alone single imaging modalities, has led to the increasing inclusion of multimodal imaging protocols in research studies and clinical trials. The combination of advanced analysis techniques and large-scale, multi-centre and data sharing initiatives is rapidly advancing the development and utility of neuroimaging biomarkers for neurodegenerative diseases.

The Alzheimer's disease Neuroimaging Initiative (ADNI) is one of the best examples of large-scale, longitudinal multi-centre studies designed to pool and share data in an effort to develop clinical, imaging, genetic and biochemical biomarkers for AD [101]. ADNI was launched in 2004 and is now in its second phase, having extended the neuroimaging protocol to include resting-state, diffusion and perfusion data. Similar efforts in other neurodegenerative diseases include the Genetic Frontotemporal Dementia Initiative (GENFI) [102] and the Parkinson's

MR Imaging Repository (PaMIR) (see [103] for a list of neuroimaging data consortia by disease). At the same time large-scale projects in healthy volunteers like the Human Connectome Project and the UK Biobank [104], as well as open repositories of neuroimaging data, are providing normative imaging data against which data from clinical populations can be compared [105]. Multicentre clinical studies such as GENFI [102] are imaging presymptomatic individuals at risk of developing FTD, with the aim of finding the earliest imaging markers of FTD, before symptom onset. In a similar vein, the UK Biobank, is collecting prospective data, imaging the brains of 100,000 people and tracking health outcomes over several decades. The multi-modal imaging data can be combined with body and cardiac imaging, genetics and lifestyle data to provide sensitive early markers for a range of diseases [104]. The integration of genetic data into neuroimaging is an important advance in the field, allowing investigation of the heritability of imaging phenotypes [105].

The availability of large datasets from clinical data sharing initiatives, advances in computing power and pattern recognition methods have led to the development of predictive modelling methods based on machine learning. These methods seek to find patterns in neuroimaging variables, such as structural or functional connectivity, that explain clinical or behavioural variables [103]. The methods enable more sensitive stratification of patients that may allow for more effective drug treatments. An ongoing challenge for the development of neuroimaging biomarkers, is the translation of complex analysis techniques to the clinic, for use on a single patient basis. Predictive modelling techniques may provide the solution by combining multiple sources of imaging, genetic and biological markers from large data sets to predict clinical outcomes in a single patient [103].

There remain significant challenges to the development and translation of neuroimaging for neurodegenerative disease. Neuroimaging methods for use as diagnostic biomarkers need to have high specificity for differential diagnosis of diseases. Biomarkers also need high sensitivity to detect pathological events before macroscale damage occurs and before symptoms are evident. To be implemented as a clinical tool there needs to be harmonisation of scanning protocols, preprocessing and analysis across centres. With the increase in neuroimaging and biomarker data collected, the ability to examine data on finer spatial scales and the pooling of data across centres, there is a need for dimensionality reduction and rigorous statistical modelling [87].

18.8 Conclusions

In this chapter, we reviewed major approaches to imaging neurodegenerative disease, demonstrating how different techniques have been used to reveal specific correlates of structural and functional dysfunction. While much progress has been achieved in improving spatial and temporal resolution, the challenge of personalised diagnosis and prognosis in neurodegeneration remains. New approaches, involving ‘big data’ and computational neuroimaging are likely to allow further advances in our understanding of neurodegeneration through neuroimaging.

Acknowledgments M.V. was supported by a grant from The Medical Research Council, project grant number MR/M023664/1. N.E. was supported by National Health and Medical Research Council project grant number APP1020526.

References

1. Ashburner J, Friston KJ (2000) Voxel-based morphometry—the methods. *NeuroImage* 11:805–821
2. Seeley WW, Crawford RK, Zhou J, Miller BL, Greicius MD (2009) Neurodegenerative diseases target large-scale human brain networks. *Neuron* 62:42–52
3. Dale AM, Fischl B, Sereno MI (1999) Cortical surface-based analysis: I. Segmentation and surface reconstruction. *Neuroimage* 9:179–194
4. Querbes O, Aubry F, Pariente J, Lotterie J-A, Démonet J-F, Duret V, Puel M, Berry I, Fort J-C, Celsis P (2009) Early diagnosis of Alzheimer’s disease using cortical thickness: impact of cognitive reserve. *Brain* 132:2036–2047
5. Du A-T, Schuff N, Kramer JH, Rosen HJ, Gorno-Tempini ML, Rankin K, Miller BL, Weiner MW (2007) Different regional patterns of cortical thinning in Alzheimer’s disease and frontotemporal dementia. *Brain* 130:1159–1166
6. Alexander-Bloch A, Giedd JN, Bullmore E (2013) Imaging structural co-variance between human brain regions. *Nat Rev Neurosci* 14:322–336
7. Evans AC (2013) Networks of anatomical covariance. *NeuroImage* 80:489–504
8. Zhou J, Gennatas ED, Kramer JH, Miller BL, Seeley WW (2012) Predicting regional neurodegeneration from the healthy brain functional connectome. *Neuron* 73:1216–1227
9. Bernhardt BC, Worsley KJ, Besson P, Concha L, Lerch JP, Evans AC, Bernasconi N (2008) Mapping limbic network organization in temporal lobe epilepsy using morphometric correlations: insights on the relation between mesiotemporal connectivity and cortical atrophy. *NeuroImage* 42:515–524
10. Reuter M, Tisdall MD, Qureshi A, Buckner RL, van der Kouwe AJW, Fischl B (2015) Head motion during MRI acquisition reduces gray matter volume and thickness estimates. *NeuroImage* 107:107–115
11. Reuter M, Fischl B (2011) Avoiding asymmetry-induced bias in longitudinal image processing. *NeuroImage* 57:19–21
12. Jones DK, Knösche TR, Turner R (2013) White matter integrity, fiber count, and other fallacies: the do’s and don’ts of diffusion MRI. *NeuroImage* 73:239–254
13. Johansen-Berg H, Behrens TEJ (2009) Diffusion MRI: from quantitative measurement to in-vivo neuroanatomy. In: *Diffus MRI*. Elsevier, Oxford. doi:10.1016/B978-0-12-374709-9.00002-X
14. Kantarci K, Avula R, Senjem ML et al (2010) Dementia with Lewy bodies and Alzheimer disease: neurodegenerative patterns characterized by DTI. *Neurology* 74:1814–1821
15. Rosas HD, Lee SY, Bender AC et al (2010) Altered white matter microstructure in the corpus callosum in Huntington’s disease: implications for cortical “disconnection.”. *NeuroImage* 49:2995–3004
16. Tournier J-D, Mori S, Leemans A (2011) Diffusion tensor imaging and beyond. *Magn Reson Med* 65:1532–1556
17. Galantucci S, Tartaglia MC, Wilson SM et al (2011) White matter damage in primary progressive aphasia: a diffusion tensor tractography study. *Brain* 134:3011–3029
18. Jeurissen B, Leemans A, Tournier J-D, Jones DK, Sijbers J (2010) Estimating the number of fiber orientations in diffusion MRI voxels: a constrained spherical deconvolution study. *Proc Int Soc Magn Reson Med* 45:3536
19. Raffelt DA, Tournier JD, Smith RE, Vaughan DN, Jackson G, Ridgway GR, Connelly A (2017) Investigating white matter fibre density and morphology using fixel-based analysis. *NeuroImage* 144:58–73

20. Harrison NA, Cooper E, Dowell NG, Keramida G, Voon V, Critchley HD, Cercignani M (2015) Quantitative magnetization transfer imaging as a biomarker for effects of systemic inflammation on the brain. *Biol Psychiatry* 78:49–57
21. Theysohn JM, Kraff O, Maderwald S, Schlamann MU, De Greiff A, Forsting M, Ladd SC, Ladd ME, Gizewski ER (2009) The human hippocampus at 7 T—in vivo MRI. *Hippocampus* 19:1–7
22. Visser F, Zwanenburg JJM, Hoogduin JM, Luijten PR (2010) High-resolution magnetization-prepared 3D-FLAIR imaging at 7.0 tesla. *Magn Reson Med* 64:194–202
23. Zwanenburg JJM, Versluis MJ, Luijten PR, Petridou N (2011) Fast high resolution whole brain T2* weighted imaging using echo planar imaging at 7T. *NeuroImage* 56:1902–1907
24. van der Kolk AG, Hendrikse J, Zwanenburg JJM, Visser F, Luijten PR (2013) Clinical applications of 7T MRI in the brain. *Eur J Radiol* 82:708–718
25. Theysohn JM, Kraff O, Maderwald S, Barth M, Ladd SC, Forsting M, Ladd ME, Gizewski ER (2011) 7 tesla MRI of microbleeds and white matter lesions as seen in vascular dementia. *J Magn Reson Imaging* 33:782–791
26. van Rooden S, Maat-Schieman MLC, Nabuurs RJA, van der Weerd L, van Duijn S, van Duinen SG, Natté R, van Buchem MA, van der Grond J (2009) Cerebral amyloidosis: post-mortem detection with human 7.0-T MR imaging system. *Radiology* 253:788–796
27. Dula AN, Virostko J, Shellock FG (2014) Assessment of MRI issues at 7 T for 28 implants and other objects. *Am J Roentgenol* 202:401–405
28. Lerch JP, van der Kouwe AJW, Raznahan A, Paus T, Johansen-Berg H, Miller KL, Smith SM, Fischl B, Sotiropoulos SN (2017) Studying neuroanatomy using MRI. *Nat Neurosci* 20:314–326
29. Bandettini PA (2009) Functional MRI limitations and aspirations. In: Kraft E, Gulyas B, Pöppel E (eds) *Neural correlates of thinking*. Springer, Berlin, pp 15–38
30. Ogawa S, Lee T-M (1990) Magnetic resonance imaging of blood vessels at high fields: in vivo and in vitro measurements and image simulation. *Magn Reson Med* 16:9–18
31. Ogawa S, Lee TM, Kay AR, Tank DW (1990) Brain magnetic resonance imaging with contrast dependent on blood oxygenation. *Proc Natl Acad Sci U S A* 87:9868–9872
32. Yacoub E, Shmuel A, Pfeuffer J, Van De Moortele PF, Adriany G, Ugurbil K, Hu X (2001) Investigation of the initial dip in fMRI at 7 Tesla. *NMR Biomed* 14:408–412
33. Amaro E, Barker GJ (2006) Study design in fMRI: basic principles. *Brain Cogn* 60:220–232
34. Abdulkadir A, Ronneberger O, Wolf RC, Pfeleiderer B, Saft C, Kloppel S (2013) Functional and structural MRI biomarkers to detect pre-clinical neurodegeneration. *Curr Alzheimer Res* 10:125–134
35. Georgiou-Karistianis N, Stout JC, Domínguez DJF et al (2014) Functional magnetic resonance imaging of working memory in Huntington's disease: cross-sectional data from the IMAGE-HD study. *Hum Brain Mapp* 35:1847–1864
36. Rosenow F, Lüders H (2001) Presurgical evaluation of epilepsy. *Brain* 124:1683–1700
37. Hage ZA, Alaraj A, Arnone GD, Charbel FT (2016) Novel imaging approaches to cerebrovascular disease. *Transl Res* 175:54–75
38. Veldsman M, Cumming T, Brodtmann A (2015) Beyond BOLD: optimizing functional imaging in stroke populations. *Hum Brain Mapp* 36:1620–1636
39. Biswal B, Yetkin FZ, Haughton VM, Hyde JS (1995) Functional connectivity in the motor cortex of resting human brain using echo-planar MRI. *Magn Reson Med* 34:537–541
40. Biswal BB, Mennes M, Zuo X-N et al (2010) Toward discovery science of human brain function. *Proc Natl Acad Sci U S A* 107:4734–4739
41. Greicius MD, Krasnow B, Reiss AL, Menon V (2003) Functional connectivity in the resting brain: a network analysis of the default mode hypothesis. *Proc Natl Acad Sci U S A* 100:253–258
42. Raichle ME, MacLeod AM, Snyder AZ, Powers WJ, Gusnard DA, Shulman GL (2001) A default mode of brain function. *Proc Natl Acad Sci U S A* 98:676–682
43. Fox MD, Snyder AZ, Vincent JL, Corbetta M, Van Essen DC, Raichle ME (2005) The human brain is intrinsically organized into dynamic, anticorrelated functional networks. *Proc Natl Acad Sci U S A* 102:9673–9678

44. Fox MD, Greicius M (2010) Clinical applications of resting state functional connectivity. *Front Syst Neurosci* 4:19
45. Petrella JR, Sheldon FC, Prince SE, Calhoun VD, Doraiswamy PM (2011) Default mode network connectivity in stable vs progressive mild cognitive impairment. *Neurology* 76:511–517
46. Greicius MD, Srivastava G, Reiss AL, Menon V (2004) Default-mode network activity distinguishes Alzheimer's disease from healthy aging: evidence from functional MRI. *Proc Natl Acad Sci U S A* 101:4637–4642
47. He BJ, Snyder AZ, Vincent JL, Epstein A, Shulman GL, Corbetta M (2007) Breakdown of functional connectivity in frontoparietal networks underlies behavioral deficits in spatial neglect. *Neuron* 53:905–918
48. Fox MD, Raichle ME (2007) Spontaneous fluctuations in brain activity observed with functional magnetic resonance imaging. *Nat Rev Neurosci* 8:700–711
49. Kiviniemi V, Kantola JH, Jauhainen J, Hyvärinen A, Tervonen O (2003) Independent component analysis of nondeterministic fMRI signal sources. *NeuroImage* 19:253–260
50. Zuo X-N, Di Martino A, Kelly C, Shehzad ZE, Gee DG, Klein DF, Castellanos FX, Biswal BB, Milham MP (2010) The oscillating brain: complex and reliable. *NeuroImage* 49:1432–1445
51. McGill ML, Devinsky O, Wang X, Quinn BT, Pardoe H, Carlson C, Butler T, Kuzniecky R, Thesen T (2014) Functional neuroimaging abnormalities in idiopathic generalized epilepsy. *NeuroImage Clin* 6:455–462
52. La C, Nair VA, Mossahebi P, Young BM, Chacon M, Jensen M, Birn RM, Meyerand ME, Prabhakaran V (2016) Implication of the slow-5 oscillations in the disruption of the default-mode network in healthy aging and stroke. *Brain Connect* 6:482–495
53. Han Y, Wang J, Zhao Z, Min B, Lu J, Li K, He Y, Jia J (2011) Frequency-dependent changes in the amplitude of low-frequency fluctuations in amnesic mild cognitive impairment: a resting-state fMRI study. *NeuroImage* 55:287–295
54. Benadiba M, Luurtsema G, Wichert-Ana L, Buchpiguel CA, Filho GB (2012) New molecular targets for PET and SPECT imaging in neurodegenerative diseases. *Rev Bras Psiquiatr.* doi:10.1016/j.rbp.2012.07.002
55. Catafau AM, Bullich S (2016) Non-amyloid PET imaging biomarkers for neurodegeneration: focus on tau, alpha-synuclein and neuroinflammation. *Curr Alzheimer Res* 14(2):169–177
56. Drzezga A, Barthel H, Minoshima S, Sabri O (2014) Potential clinical applications of PET/MR imaging in neurodegenerative diseases. *J Nucl Med* 55:47–55
57. Zhu L, Ploessl K, Kung HF (2014) PET/SPECT imaging agents for neurodegenerative diseases. *Chem Soc Rev* 43:6683–6691
58. Kadir A, Nordberg A (2010) Target-specific PET probes for neurodegenerative disorders related to dementia. *J Nucl Med* 51:1418–1430
59. Mosconi L, Tsui WH, Herholz K et al (2008) Multicenter standardized 18F-FDG PET diagnosis of mild cognitive impairment, Alzheimer's disease, and other dementias. *J Nucl Med* 49:390–398
60. Landau SM, Harvey D, Madison CM, Koeppe RA, Reiman EM, Foster NL, Weiner MW, Jagust WJ (2011) Associations between cognitive, functional, and FDG-PET measures of decline in AD and MCI. *Neurobiol Aging* 32:1207–1218
61. Villemagne VL, Doré V, Bourgeat P, Burnham SC, Laws S, Salvado O, Masters CL, Rowe CC (2017) A β -amyloid and tau imaging in dementia. *Semin Nucl Med* 47:75–88
62. Shah M, Catafau AM (2014) Molecular imaging insights into neurodegeneration: focus on tau PET radiotracers. *J Nucl Med* 55:871–874
63. Holman BL, Carvalho PA, Mendelson J, Teoh SK, Nardin R, Hallgring E, Hebben N, Johnson KA (1991) Brain perfusion is abnormal in cocaine-dependent polydrug users: a study using technetium-99m-HMPAO and ASPECT. *J Nucl Med* 32:1206–1210
64. Karonen JO, Nuutinen J, Kuikka JT, Vanninen EJ, Vanninen RL, Partanen PLK, Vainio PA, Roivainen R, Sivenius J, Aronen HJ (2000) Combined SPECT and diffusion-weighted MRI as a predictor of infarct growth in acute ischemic stroke. *J Nucl Med* 41:788–794

65. Benamer HTS, Uk M, Patterson J, Grosset DG, Joseph K, Tatsch K, Schwarz J, Ries V (2000) Accurate differentiation of parkinsonism and essential tremor using visual assessment of [¹²³I]-FP-CIT SPECT imaging : the [¹²³I]-FP-CIT study group. *Mov Disord* 15:503–510
66. Loos C, Achten E, Santens P (2010) Proton magnetic resonance spectroscopy in Alzheimer's disease, a review. *Acta Neurol Belg* 110:291–298
67. Kantarci K, Weigand SD, Petersen RC et al (2007) Longitudinal 1H MRS changes in mild cognitive impairment and Alzheimer's disease. *Neurobiol Aging* 28:1330–1339
68. Adalsteinsson E, Sullivan EV, Kleinhans N, Spielman DM, Pfefferbaum A (2000) Longitudinal decline of the neuronal marker N-acetyl aspartate in Alzheimer's disease. *Lancet* 355:1695–1696
69. Voevodskaya O, Sundgren PC, Strandberg O, Zetterberg H, Minthon L, Blennow K, Wahlund LO, Westman E, Hansson O (2016) Myo-inositol changes precede amyloid pathology and relate to APOE genotype in Alzheimer disease. *Neurology* 86:1754–1761
70. Murray ME, Przybelski SA, Lesnick TG et al (2014) Early Alzheimer's disease neuropathology detected by proton MR spectroscopy. *J Neurosci* 34:16247–16255
71. Wilson TW, Heinrichs-Graham E, Proskovec AL, McDermott TJ (2015) Neuroimaging with magnetoencephalography: a dynamic view of brain pathophysiology. *Transl Res* 175:17–36
72. Luck SJ (2005) An introduction to the event-related potential technique. MIT Press Ltd, Cambridge
73. Grynszpan F, Geselowitz DB (1973) Model studies of the magnetocardiogram. *Biophys J* 13:911–925
74. Cuffin N, Cohen D (1979) Comparison of the magnetoencephalogram and electroencephalogram. *Electroencephalogr Clin Neurophysiol* 47:132–146
75. Juckel G, Clotz F, Frodl T, Kawohl W, Hampel H, Pogarell O, Hegerl U (2008) Diagnostic usefulness of cognitive auditory event-related p300 subcomponents in patients with Alzheimers disease? *J Clin Neurophysiol* 25:147–152
76. Papadaniil CD, Kosmidou VE, Tsolaki A, Kompatsiaris IY, Hadjileontiadis LJ (2016) Cognitive MMN and P300 in mild cognitive impairment and Alzheimer's disease: a high density EEG-3D vector field tomography approach. *Brain Res* 1648:425–433
77. Tallon-Baudry C, Bertrand O (1999) Oscillatory gamma activity in humans and its role in object representation. *Trends Cogn Sci* 3:151–162
78. Uhlhaas PJ, Haenschel C, Nikolić D, Singer W (2008) The role of oscillations and synchrony in cortical networks and their putative relevance for the pathophysiology of schizophrenia. *Schizophr Bull* 34:927–943
79. Gevins A, Smith ME, McEvoy L, Yu D (1997) High-resolution EEG mapping of cortical activation related to working memory: effects of task difficulty, type of processing, and practice. *Cereb Cortex* 7:374–385
80. Klimesch W (2012) Alpha-band oscillations, attention, and controlled access to stored information. *Trends Cogn Sci* 16:606–617
81. Buzsáki G, Draguhn A (2004) Neuronal oscillations in cortical networks. *Science* 304:1926–1929
82. Stoffers D, Bosboom JLW, Deijen JB, Wolters EC, Stam CJ, Berendse HW (2008) Increased cortico-cortical functional connectivity in early-stage Parkinson's disease: an MEG study. *NeuroImage* 41:212–222
83. Stam CJ (2010) Use of magnetoencephalography (MEG) to study functional brain networks in neurodegenerative disorders. *J Neurol Sci* 289:128–134
84. Greicius M, Seeley W, Carter AR, Shulman GL, Corbetta M (2012) Why use a connectivity-based approach to study stroke and recovery of function? *NeuroImage* 62:2271–2280
85. Smith SM, Beckmann CF, Andersson J et al (2013) Resting-state fMRI in the Human Connectome Project. *NeuroImage* 80:144–168
86. Union E (2014) The human brain project—human brain project. *Hum Brain Proj Website*. 50–55
87. Bassett DS, Sporns O (2017) Network neuroscience. *Nat Neurosci* 20:353–364

88. Bullmore E, Sporns O (2009) Complex brain networks: graph theoretical analysis of structural and functional systems. *Nat Rev Neurosci* 10:186–198
89. Crossley NA, Mechelli A, Scott J, Carletti F, Fox PT, McGuire P, Bullmore ET (2014) The hubs of the human connectome are generally implicated in the anatomy of brain disorders. *Brain*. doi:10.1093/brain/awu132
90. Buckner RL, Sepulcre J, Talukdar T, Krienen FM, Liu H, Hedden T, Andrews-Hanna JR, Sperling RA, Johnson KA (2009) Cortical hubs revealed by intrinsic functional connectivity: mapping, assessment of stability, and relation to Alzheimer's disease. *J Neurosci* 29:1860–1873
91. Fornito A, Bullmore ET, Zalesky A (2017) Opportunities and challenges for psychiatry in the connectomic era. *Biol Psychiatry Cogn Neurosci Neuroimaging* 2:9–19
92. Perlmutter JS, Mink JW (2006) Deep brain stimulation. *Annu Rev Neurosci* 29:229–257
93. Bronstein JM, Tagliati M, Alterman RL et al (2011) Deep brain stimulation for Parkinson disease. *Arch Neurol* 68:165–165
94. Delorme C, Rogers A, Lau B, Francisque H, Welter M-L, Vidal SF, Yelnik J, Durr A, Grabli D, Karachi C (2016) Deep brain stimulation of the internal pallidum in Huntington's disease patients: clinical outcome and neuronal firing patterns. *J Neurol* 263:290–298
95. Edwards TC, Zrinzo L, Limousin P, Foltynie T (2012) Deep brain stimulation in the treatment of chorea. *Mov Disord* 27:357–363
96. Sankar T, Chakravarty MM, Bescos A et al (2015) Deep brain stimulation influences brain structure in Alzheimer's disease. *Brain Stimul* 8:645–654
97. Parkin BL, Ekhtiari H, Walsh VF (2015) Non-invasive human brain stimulation in cognitive neuroscience: a primer. *Neuron* 87:932–945
98. Vallence AM, Ridding MC (2014) Non-invasive induction of plasticity in the human cortex: uses and limitations. *Cortex* 58:261–271
99. Hoyer EH, Celnik PA (2011) Understanding and enhancing motor recovery after stroke using transcranial magnetic stimulation. *Restor Neurol Neurosci* 29:395–409
100. Lefaucheur J-P, André-Obadia N, Antal A et al (2014) Evidence-based guidelines on the therapeutic use of repetitive transcranial magnetic stimulation (rTMS). *Clin Neurophysiol* 125:2150–2206
101. Jack CR, Bernstein MA, Fox NC et al (2008) The Alzheimer's Disease Neuroimaging Initiative (ADNI): MRI methods. *J Magn Reson Imaging* 27:685–691
102. Rohrer JD, Nicholas JM, Cash DM et al (2015) Presymptomatic cognitive and neuroanatomical changes in genetic frontotemporal dementia in the genetic frontotemporal dementia initiative (GENFI) study: a cross-sectional analysis. *Lancet Neurol* 14:253–262
103. Woo C-W, Chang LJ, Lindquist MA, Wager TD (2017) Building better biomarkers: brain models in translational neuroimaging. *Nat Neurosci* 20:365–377
104. Miller KL, Alfaro-Almagro F, Bangarter NK et al (2016) Multimodal population brain imaging in the UK Biobank prospective epidemiological study. *Nat Neurosci* 19:1523–1536
105. Bandettini P, Bullmore E (2012) The future of functional MRI in clinical medicine. *NeuroImage* 62:1267–1271